AIAA 2000-0360

Effect of Ice Accretion on Aircraft Flight Dynamics

M.B. Bragg, T. Hutchison, J. Merret, R. Oltman, and D. Pokhariyal
University of Illinois at Urbana-Champaign
Urbana, IL 61801

38th AIAA Aerospace Sciences Meeting & Exhibit
January 10-13, 2000 / Reno, NV

Effect of Ice Accretion on Aircraft Flight Dynamics

M. B. Bragg[†], T. Hutchison[*], J. Merret[*]
R. Oltman[*], and D. Pokhariyal[*]

University of Illinois at Urbana-Champaign

ABSTRACT

The effect of ice accretion was modeled on the performance and control of an aircraft. A simple method was presented to alter the aircraft stability and control parameters to model the effect of ice accretion. A six degree-of-freedom computational flight dynamics model was used to study the effect of the ice accretion on the aircraft dynamics including the effect of atmospheric turbulence and sensor noise. This study is part of a larger research program to develop smart icing system technology. The goal of the study reported here was to develop techniques to sense the effect of ice accretion on the aircraft performance and control during quasi-steady-state flight. A simple model to relate ice accretion effects to icing and flight parameters is proposed. The computational model showed large changes in V, α, and δ_e as the ice accretes for a constant power and altitude case. Atmospheric turbulence and sensor noise are modeled and a filter is shown to remove most of these effects. Aircraft operated at constant velocity show smaller effects and aerodynamic sensors are proposed to aid in the characterization of these cases.

LIST OF SYMBOLS AND ABBREVIATIONS

A_c	accumulation parameter
$C_{(A)}$	arbitrary performance or stability and control derivative
C_d	airfoil drag coefficient
C_{D0}	aircraft drag coefficient for zero lift coefficient
C_{m_α}	variation of pitching moment coefficient with angle of attack
C_{n_β}	weathercock stability
$C_{n_{\delta r}}$	rudder effectiveness
FDC	Flight Dynamics Code
E	collection efficiency
g	acceleration due to gravity
h	altitude
IMS	Ice Management System
IPS	Icing Protection System
k_{C_A}	coefficient icing factor constant
k'_{C_A}	coefficient icing factor
K_0	modified inertia parameter
LWC	Liquid Water Content
MVD	Median Volumetric Diameter
n	freezing fraction
SIS	Smart Icing System
T	atmospheric air temperature
t	time
TIP	Tailplane Icing Program
V	aircraft, freestream velocity
Δ	change
α	angle of attack
δ_e	elevator deflection
η	aircraft icing parameter
η_{ice}	icing severity parameter
ρ_{ice}	density of ice

1.0 INTRODUCTION

Aircraft accidents continue to occur due to the formation of ice on aircraft in flight. The primary cause of these accidents is the effect of ice on aircraft control.[1] Icing accidents can be prevented in two different ways: 1) Icing conditions can be avoided, or 2) the aircraft system can be designed and operated in an ice tolerant manner. For all aircraft, ice avoidance is a desirable goal for increased safety. However, for commercial aircraft, where revenue and schedules must be maintained, ice tolerance will continue to be the preferred method for all but the most severe icing conditions. Our approach is to conduct research to

[†] Professor and Head, Department of Aeronautical and Astronautical Engineering, Associate Fellow AIAA.
[*] Graduate Research Assistant, Department of Aeronautical and Astronautical Engineering, Member AIAA.

improve the safety of operations in icing conditions (ice tolerance) by developing the Smart Icing Systems (SIS) concept through an interdisciplinary systems approach.

Successful ice tolerant concepts were first applied to aircraft in the 1930's with the installation of pneumatic boots on aircraft wings. Since that time, ice tolerant aircraft icing research has focused on sensing ice, improved ice removal methods, ice physics and other very specific research areas. Only very recently has icing research begun to focus on safety in terms of an overall systems view of the problem. Particularly lacking is the application of flight mechanics, aircraft control and human factors to the icing safety problem. Recent advances in digital control, cockpit instrumentation and computer-based automation make it possible to develop new approaches to ice tolerant aircraft design and operation.

The important effect of ice on an aircraft is its influence on the performance, stability and control of the aircraft system. Safety will be achieved in an ice tolerant aircraft if the pilot/aircraft system can continue to maintain the desired flight path, with an acceptable safety margin, regardless of atmospheric icing conditions. One scenario for a modern approach to an ice tolerant aircraft is:

1. Sense the effect of ice accretion on aircraft performance, stability and control. Sense ice accretion and ice protection system performance. Provide the appropriate information to the flight crew.
2. Automatically activate and manage the ice protection systems, and provide the pilot with feedback on the system status and behavior of both the aircraft and the ice protection system.
3. Modify the aircraft flight envelope by use of the flight control system to avoid conditions where flight could potentially be uncontrollable. Notify the flight crew of this action and its implications for the flight envelope.
4. Adapt the aircraft control laws to maintain clean-aircraft-like flying qualities to enable the aircraft to be safely flown within the reduced flight envelope. Notify the flight crew of this action and maintain good pilot-automation coordination.

Such a smart icing systems concept could potentially contribute to a significant reduction in aircraft icing accidents and fatalities.[2]

Currently an interdisciplinary team of researchers from the University of Illinois at Urbana-Champaign is conducting the fundamental research necessary to develop a smart icing system as described above. Bragg et al.[3] in 1998 described the basics of the research program and its motivation. The control center of the envisioned smart icing system would be the ice management system (IMS) that would perform the 4 functions of: characterization, ice protection system (IPS) operation, envelope protection and control adaptation as described above and depicted in Fig. 1. Three research teams (Aerodynamics and Flight Mechanics, Controls and Sensors, and Human Factors) are conducting the research to develop the IMS. In addition, teams are also conducting a Safety and Economics Trade Study[2] to assess the potential impact of technology and developing a piloted flight simulator to serve as a systems integrator to evaluate the technical merit of the system.

The aerodynamics and flight mechanics group is responsible for providing accurate and robust models of the effect of ice on aircraft flight mechanics. These models are critical to the development of the IMS and the flight simulation capability. As part of the IMS development, these models are used for research on dynamic parameter estimation techniques that are an important part of the ice effects characterization function. Initial results of this research were reported by Melody et al.[4]

In this paper, a simple model is presented to include the effect of ice on linear and nonlinear aircraft stability and control derivatives. This technique is used in conjunction with a six degree-of-freedom computational flight mechanics model to study the effects of ice on aircraft dynamics. Also using this model, the effect of ice accretion on steady-state parameters, such as angle of attack and elevator deflection angle, are studied. These effects and others are evaluated for possible use in detecting the effect of ice accretion in flight when insufficient dynamic content, such as an elevator doublet, is available to use system identification techniques.

2.0 THEORETICAL AND COMPUTATIONAL METHODS

In this section the theoretical and computational methods used are described. First, a brief review of prior experimental research where icing effects, including stability and control parameters, were measured on natural and simulated iced aircraft is presented. A review of earlier computational methods is also included. Then, the aircraft models for an iced aircraft used in this study are presented. Finally, the computational method used to model the aircraft dynamics is described and validated.

2.1 Review of Previous Research

Of the early work that contained quantitative flight mechanics results, the primary measurements were of aircraft performance. One of the earliest successful attempts to measure the effect of ice accretion on aircraft was that of Preston and Blackman[5] in 1948.

One flight encountered a Liquid Water Content LWC = 0.4 g/m^3, Median Volumetric Diameter MVD = 17 μm and 50 min duration that resulted in an 81% increase in parasite drag and the "control response of the airplane approached the point of being marginal."

The effect of ice on the performance of high performance piston-propeller general aviation aircraft has been presented by Leckman.[6] Calculated performance for a Cessna Centurion and Skymaster in continuous maximum conditions were presented along with some flight data at various icing conditions. Leckman estimated for the Centurion a drag coefficient rise of ΔC_{D0} = 0.055 (275% increase) with no ice protection and 0.0179 (90% increase) with the ice protection system operating due to residual ice and unprotected surfaces. These estimates are for a severe, worst case encounter of glaze ice at LWC = 0.46 g/m^3, MVD = 20 μm for 200 miles which corresponded to about 1 inch of ice on the wings. Lift was also affected. Flight test data with ¼ inch rough glaze ice increased the stall speed from 75 mph clean to 102 mph at zero flap deflection and from 65 to 83 mph at 30 degrees flap deflection. Flight data on the Skymaster was presented for several ice thicknesses.

Ashenden and Marwitz[7] have compiled the data for over 20 years of operation of a Beech King Air in icing conditions. The aircraft was equipped for performance measurements and was fully instrumented to obtain meteorological data. Twenty five flights were summarized and some analyzed in more detail. Drag was found to increase by as much as 200% and increases of 50% were common. The most severe conditions were found to be freezing drizzle encounters. The rate of performance degradation was found to be the best indicator of the severity of the icing encounter.

By far the largest flight data set in icing has been obtained by NASA Glenn Research Center on the Twin Otter aircraft. Initially the research reported the effect of natural icing encounters on aircraft performance.[8,9,10] For example, Ranaudo et al.[10] have reported very carefully obtained performance flight test results for two natural icing encounters. In one encounter for 45 minutes at 131 kts with average cloud properties of LWC = 0.20 g/m^3, temperature of -5.3° C and MVD = 15 μm a significant loss in lift curve slope (8%) was measuered. Also, C_{D0} increased by about 60% for the all iced case and 17% for the case where all the ice protection was used. Therefore, for this case almost 30% of the drag rise was from miscellaneous non-ice protected components. A slight increase in the slope of the curve with ice indicates that the drag due to lift increased as ice was accreted. This effect became more pronounced at the lower power setting.

Most significant to this research were the measurements of the effect of natural and simulated ice accretion on the Twin Otter stability and control by Ranaudo et al.[10,11] and Ratvasky and Ranaudo.[12] Parameter identification methods were used to determine the stability derivatives of the aircraft with and without ice. Early research used the modified maximum likelihood estimate method, MMLE, and the subsequent data were reduced using modified stepwise regression, MSR. In both techniques, control inputs in the form of doublets were executed, and the inputs and aircraft response were recorded digitally. After several repeat runs the data were processed to determine the stability derivatives, when used in the equations of motion, that best predict the measured responses. The effect of power, landing flaps and angle of attack were studied to determine under what conditions the effect of the ice was most significant.

The effect of a simulated moderate glaze ice accretion attached to the horizontal and vertical tail was determined.[12] The no flap case at low power setting reduced the longitudinal static stability by increasing C_{m_α} by approximately 10%. This reduction in stability was true for all iced cases and rose to 17% for the flap deflected 10° case and no power. As expected the presence of ice on the tail reduced the effectiveness of the elevator. A reduction of 12% was measured for the no flap case, which was shown to increase to 16% with 10° of flaps. Earlier measurements[10] in natural ice showed a 15% reduction in elevator effectiveness with all the aircraft iced, which reduced to about 9% when all but the tail was deiced. Thus the numbers quoted above may have been larger had simulated ice been used on the entire aircraft.

Lateral stability and control were also affected by ice and Ratvasky and Ranaudo[12] studied the effect of simulated tail ice on these parameters. Weathercock stability, C_{n_β}, was reduced, particularly at the no power condition. Rudder effectiveness, $C_{n_{\delta_r}}$, was reduced by approximately 8% by the simulated moderate glaze ice tested on the tail surfaces.

Control issues also arise due to the effect ice has on aerodynamic hinge moments and, therefore, stick forces for aircraft with unpowered controls.[13] Trunov and Ingelman-Sundberg[14] presented an excellent discussion of the role of the change in elevator hinge moment in the horizontal tail stall with icing accidents. Lower surface separation on the tail led to the loss of effectiveness and a large change in hinge moment that can overpower the pilot. This resulted from the downwash at the tail experienced with the use of high-powered landing flaps. Tailplane stall and the FAA pushover maneuver have been the topic of a recent extensive NASA research program on the Twin Otter.[15] The focus of this effort was to improve the understanding of tailplane stall, develop analytical tools, and develop training aides for pilots.

As a result of the NASA Twin Otter research briefly reviewed here, it is clear that ice accretion affects the longitudinal and lateral static stability and control of the aircraft. This effect occurs even at low angle of attack and high power setting, conditions typical of cruise. A typical reduction in stability or control was 10%. Most of these data come from tail only simulated ice and the authors commented that these effects may be even more significant on other aircraft which do not have a large, oversized tail such as that on the Twin Otter.[12] There is also evidence that the effects of ice are more significant at large angles of attack near stall where significant early flow separation occurs due to the ice.[14]

Several researchers have simulated the effect of ice accretion on aircraft dynamics using computer models. Karlsen and Solberg[16] simulated the approach to landing of a light transport aircraft with horizontal tail ice. The simulations showed that icing leads to partial tailplane stall induced by the aircraft pitching motion. A simple glideslope controller was also used that showed that the aircraft might become unstable using a controller tuned for the clean aircraft dynamics.

As part of the NASA/FAA Tailplane Icing Program Hiltner[17] performed a nonlinear aircraft simulation of ice contaminated tailplane stall. Hiltner developed a nonlinear model of the NASA Twin Otter aircraft with horizontal tailplane ice using flight test and wind tunnel data. The pushover maneuver was modeled and all zero g cases, with nonzero flap deflections and ice, showed a tendency for control difficulties. These difficulties included inadequate flying qualities if the tailplane angle of attack exceeded the angle for the hinge moment break and reduced stability near tail stall. Miller and Ribbens[18] used systems identification techniques to analyze the NASA tailplane icing data and then applied these models to explore the use of elevator effectiveness as an icing detector.[19]

2.2 Iced Aircraft Model Development

As seen in the review above, only a few natural icing encounters have been studied to obtain stability and control derivatives. Acquiring these data from flight test is expensive and time consuming, thus no database of effects versus icing conditions are available. However, for the overall smart icing research program it is important to have an aircraft model that reflects the change with icing conditions. Therefore, in this section such a model is presented. Several researchers have attempted to fit airfoil drag and lift as a function of icing conditions. For various reasons, the accuracy of even these relatively simple models is low. Therefore, it is recognized that the absolute accuracy of this model is probably low as well, but the intent is to reasonably simulate some of the important trends in aircraft performance and control with icing parameters.

The objective of the icing effects model is to devise a simple, but physically representative, model of the effect of ice on aircraft flight mechanics for use in the characterization and simulation required for the development of the Smart Icing System. The icing effects model is based on the following equation

$$C_{(A)iced} = (1 + \eta_{ice}\, k'_{C_A})\, C_{(A)}$$

In this equation, η_{ice} is an icing severity parameter, and represents the amount and severity of the icing encounter. η_{ice} is defined such that it is not a function of the aircraft, only the atmospheric conditions. k'_{C_A} is the coefficient icing factor that depends the coefficient being modified and the aircraft specific information. Here the k'_{C_A} term accounts for one aircraft due to its size, speed, or design being more susceptible to icing than another aircraft. $C_{(A)}$ is any arbitrary performance, stability or control parameter or derivative that is affected by ice accretion.

In this preliminary formulation, the weighting factor, k'_{C_A}, is assumed to be a function of several parameters where k'_{C_A} = f(IPS, aircraft geometry and configuration, icing conditions) and IPS refers to the status and activity of the Icing Protection System.

Similarly, the icing severity parameter, η_{ice}, as currently formulated is a function of two parameters

$$\eta_{ice} = f(n, A_c E)$$

Where n is the freezing fraction, A_c is the accumulation parameter, and E is the collection efficiency. The icing severity parameter η_{ice} is intended to represent the severity of an icing parameter in terms of the flight mechanics of an aircraft. However, since the greatest amount of ice accretion effects data were available for the drag of a NACA 0012 airfoil, this is used to define η_{ice} as described below.

In simplest terms, n is the fraction of water freezing at a point on a surface to the water impinging on the surface.

$$n = \frac{mass\ of\ water\ freezing}{mass\ of\ water\ impinging}$$

Inherent in the freezing fraction value is the type of ice that forms. A high freezing fraction, close to unity, indicates rime ice formation, while a lower freezing fraction indicates glaze ice formation. A simple method based on the work of Cook,[20] that calculates n

at the stagnation point of a cylinder was used to generate n.

The accumulation parameter, A_c, is a nondimensional mass flux and can be thought of as the length of ice growth in airfoil chords that would form on an imaginary flat plate placed perpendicular to the freestream flow for a time t, and it is defined as follows:

$$A_c = \frac{V(LWC)t}{\rho_{ice}c}$$

Where V is the freestream velocity, LWC is the liquid water content of the freestream, t is the time of exposure, ρ_{ice} is the density of ice, and c is the chord length of the airfoil. One aspect of the accumulation parameter makes it particularly useful is the ability of the parameter to account for exposure time through the t term.

The final parameter is the collection efficiency, E, which is defined as follows:

$$E = \frac{mass\ of\ water\ droplets\ impinging}{mass\ of\ water\ seen\ in\ the\ body\ projected\ area}$$

In this formulation of η_{ice}, ΔC_d data were taken from NASA Icing Research Tunnel data of Olsen, Shaw and Newton[21] and were curve fit as a function of A_cE and freezing fraction. From the data of Olsen et al. it is seen that the drag peaks at about $n = 0.2$ and decreases as the freezing fraction deviates from this value. Figure 2 is a plot of the increase in airfoil drag and predicted values versus the freezing fraction for two different A_cE values. As n increases from 0.2 the ice becomes more rime like and in general the drag decreases due to the reduction and ultimate disappearance of the upper surface horn. As n decreases from 0.2, less of the impinging water freezes, causing a reduction in the amount of ice accretion and a decrease in the drag. At $n = 0$ no ice forms on the airfoil (at least at the stagnation point where n is calculated and this simple model assumes this applies to the entire airfoil) and the drag rise is zero.

The equation for the ΔC_d curves has the following general form:

$$\Delta C_d = Z_1 \cdot (A_cE) \cdot g(n)$$

Where Z_1 is a constant, and the function g varies linearly with n, peaking at a value of 0.2. Based on the data presented by Olsen et al.[21] and Bowden[22] the ΔC_d curves were constructed to vary linearly with the value of A_cE. This means that ΔC_d increases linearly with time as is apparent in particularly the glaze ice data on a NACA 0011 airfoil from Bowden.[22] Figure 3 is a plot of the ΔC_d experimental data and calculated values versus A_cE for various values of n. The linear variation with A_cE is apparent, along with the maximum of ΔC_d at n=0.2. Figure 4 is a plot of the airfoil drag data presented by Olsen et al.[21] versus the calculated drag values. The line in Fig. 4 represents perfect agreement between the experimental and calculated values.

In order to nondimensionalize the ΔC_d equation to form the η_{ice} parameter, a reference condition was chosen based loosely on FAA Appendix C maximum continuous conditions on a 3 foot chord NACA 0012 airfoil (MVD = 20 μm, V_∞ = 175 knots, LWC = 0.65 g/m^3, t = 10 min, T_0 = 25 °F). Hence, the η_{ice} equation was defined as follows:

$$\eta_{ice} = \frac{\Delta C_d(NACA\ 0012, c = 3', V = 175kts.actual.conditions)}{\Delta C_{d_{ref}}(NACA\ 0012, c = 3', cont.\ \max.conditions)}$$

Unfortunately, this simple formulation for η_{ice}, does not sufficiently capture aircraft dependent properties to allow for an accurate determination of iced coefficient values. In order to account for these aircraft dependencies, it was necessary to define k'_{C_A} as follows:

$$k'_{C_A} = \frac{\eta}{\eta_{ice}} k_{C_A}$$

In this formulation, the η_{ice} value is calculated as above, using a 3 foot chord NACA 0012 airfoil at 175 knots. Here η, the aircraft icing parameter, is calculated in the same way as η_{ice} except the chord and velocity corresponding to the aircraft and conditions being examined are used in the numerator. The k_{C_A} represents the change in an aircraft parameter C_A, that is constant for a given aircraft. By using this formulation, the aircraft specific chord, airfoil, and velocity are adequately captured, allowing for a more accurate determination of iced coefficient values.

The η_{ice} formulation is far from complete, as there are still a sufficient number of improvements to be made to the model. Initially, more data needs to be collected from other sources and integrated into the model. Once the model has been developed further, the possibility of including other independent variables will be examined. One variable that is already being considered is K_0, the modified inertia parameter.

2.3 Clean and Iced Aircraft Models

The current longitudinal and lateral aircraft flight dynamics model was obtained from published NASA Twin Otter flight results. The results obtained from the

Twin Otter flight with simulated tailplane icing were used to estimate most of the derivatives.[11,12] The drag and other non-tail related derivatives were obtained from flight test results in which the entire aircraft was subjected to icing.[10] Where values were not available, they were estimated. A comparison of the clean and iced derivatives is shown in Table 1. Also shown is a simple model of only horizontal tail icing and only wing icing derived from these same data. The derivatives are representative of icing conditions that yield η=0.2. From these data the k_{C_A} values are derived for use in the icing model. The model outlined in Table 1 is used to represent the derivatives in all flight conditions, i.e. there is no dependence of the derivatives on flight variables such as angle of attack and velocity. This model was intended primarily for use in the quasi-steady analysis performed in this paper.

The use of Digital DATCOM[23] to determine the derivatives of the Twin Otter as a function of angle of attack has been implemented and is being explored as an inexpensive alternative to flight test data. The DATCOM model is currently only for the clean aircraft case and the derivatives vary with angle of attack making the model fully nonlinear. The derivatives generated by Miller and Ribbens[18] are also used to validate the Flight Mechanics Code being used. This model was derived using system identification methods from the NASA/FAA TIP data.

2.4 Flight Mechanics Code

The flight analysis of the clean and iced aircraft models were carried out using a Flight Dynamics and Control (FDC) toolbox for MATLAB & Simulink.[24] The FDC code solves 12 coupled nonlinear differential equations to describe the aircraft's dynamic motion using control surface deflections, power, etc. as inputs. The FDC also incorporates an atmospheric turbulence model based on the NASA Dryden wind gust model. The onset and accumulation of icing are modeled into the FDC code during flight by modifying the derivatives at each time step. Various flight models can be incorporated into the FDC code and used to simulate aircraft flight. The FDC code is modified as required and simulations are carried out in the open loop and autopilot modes. The code has also been updated to include sensor noise.

A validation of the FDC code was carried out by comparing the present results obtained with the FDC to those obtained by the method of Miller and Ribbens[18] to TIP flight p5220. The FDC code was run in an open loop scenario using the actual elevator input from TIP flight p5220 (no ice). The response of the various Twin Otter models to the p5220 input doublet of the same shape, but shifted to take into account the different trim conditions, are explored. Figure 5 shows the elevator doublets used in the TIP flight and in this simulation.

The simulations are conducted at the same constant power setting. The aircraft is trimmed at an altitude of 5620 ft and a velocity of 188 ft/s before the doublet is applied.

Figure 6 shows the measured and predicted clean aircraft response in velocity, altitude and angle of attack to the input elevator doublet. The Miller and Ribbens curve uses the stability and control parameters they generated from the TIP data set in our FDC code. The comparison to the TIP data is quite good, as would be expected, and validates the dynamics of the FDC code. The DATCOM model uses only aircraft geometry to generate its aircraft stability and control model. In addition, it interpolates the derivatives between angle of attack values in a "look-up table" method. The DATCOM does not compare as well as the Miller and Ribbens model, but the results are acceptable. The Twin Otter model used for the calculations in this report is shown as the "Current Steady-State Model" in Fig. 6. This model is based on the actual measured derivatives from earlier flight tests. The comparison to the measured elevator doublet response is acceptable, but it underpredicts the response. This is probably due to a reduced elevator power and a larger pitch-damping derivative in the current model as compared to the Miller and Ribbens model. However, the values used in the current model are more representative of those measured on the Twin Otter, and since the dynamic response was not an important part of this study, the current model was used without modification.

3.0 RESULTS AND DISCUSSION

3.1 Effect of Ice Accretion

Through the use of the η and η_{ice} the effect of varying icing cloud conditions on aircraft performance and control can be predicted. Figure 7 shows the variation of η with static temperature, LWC, and droplet size. Note that η is shown and not η_{ice}. Here η was calculated for the Twin Otter about the following baseline conditions:

Altitude = 9000 ft
Velocity = 269 ft/s (159 kts)
LWC = 0.65 g/m^3
MVD = 20 μm
T = 25°F
t = 5 minutes

The η values are significantly smaller than the corresponding η_{ice} values due to the larger chord of the Twin Otter airfoil (6.6 ft.) than the reference chord of 3 ft. used in η_{ice}.

Figure 7 a) shows η versus *LWC* for 5 different static air temperatures. These plots can best be interpreted by understanding the relationship between *AcE* and n to the cloud parameters. *AcE* increases linearly with increasing *LWC* in the current η formulation. Also, η increases linearly with n until n = *0.2*, then decreases linearly from that point. For the T = *29°F* case η increases rapidly until *LWC* = *0.2* then increases at a lower rate. The change in the slope of the curve corresponds to where n = *0.2*. Beyond this *LWC*, n is decreasing but *AcE* is increasing faster, so a small increase in η with *LWC* is seen beyond this point. The T = *25°F* case behaves in a similar manner but breaks at a higher *LWC* value. At T = *20°F*, η is almost constant from zero to 0.2 *LWC*. In this range n = *1.0*. For *LWC* > *0.2*, n is decreasing and η grows rapidly as a result. Above *LWC* = *1.4*, η grows more slowly as n reaches 0.2 and decreases. T = *10°F* and *20°F* curves behave similarly. First growing slowly as n = *1.0*, then rapidly as the increased *LWC* reduces the freezing fraction.

Similar trends are seen in Figs. 7 b) and c). In Fig. 7 b) the peak η values occur at temperatures corresponding to n = *0.2*. As the *LWC* increases, this temperature decreases as seen in the figure. The *LWC* = *0.2* curve is constant up to a temperature of almost 20°F. In this temperature range n = *1.0* at this low *LWC* and since only T is varying, *AcE* is constant and therefore η is constant as well. Finally, Fig. 7 c) shows the effect of droplet size on η. As the droplet size increases, η is affected both through the *AcE* term and n. Increasing droplet size increases the collection efficiency E increasing the amount of water impinging and as a result increasing the amount of ice. This increased water load also reduces the freezing fraction n. Thus for cold temperatures and low droplet size n = 1.0 and the increase in η with droplet size is small. At a certain droplet size that decreases with increasing temperature, η starts to increase more rapidly as n decreases toward glaze accretions. For T = 25°F and 29°F the increase in η with droplet size is reduced as n is less than 0.2.

Figures 8 a), b), and c) reflect the predicted change in Twin Otter cruise performance due to the icing effects with static temperature as predicted in Fig. 7 a). The Flight Dynamics code was run for a cruise case with constant altitude (9000 ft.) and aircraft power. The aircraft parameters were changed with time to simulate a 5 minute icing encounter during which the ice protection system was not operated.

In Fig. 8 a) the change in velocity with time is shown for the 5 different static air temperatures. The temperatures are shown in the legend in the order of increasing η and, therefore, increasing aircraft performance penalty. For example, for the temperatures 29, 0, 10, 25, and 20°F, the corresponding η values at 5 minutes (300 secs) are 0.012, 0.032, 0.081, 0.094, and 0.12, respectively. Note that the nominal η value for the Twin Otter flights on which the iced aircraft model was based was 0.10. The large reduction in airspeed is a direct result of the significant drag rise due to the ice accretion. This is particularly true at static air temperatures of 10, 20 and 25°F where the model predicts high-drag glaze formations. For example at 20°F and 300 seconds of ice accretion, the model predicts a velocity of 206 ft/s from the clean value of 269 ft/s, a 23% loss in airspeed. At the very cold or warm temperatures the loss is much less.

Figures 8 b) and c) show the predicted change in aircraft angle of attack, α, and elevator angle, δ_e, versus time. The large changes shown are due to 2 primary factors: 1) as the drag slows the aircraft operated at constant power, the aircraft rotates to a higher α to maintain lift and as a result a larger δ_e is required to trim, and 2) The ice degrades the aircraft lift curve slope and elevator effectiveness requiring larger α and δ_e to trim. As in Fig. 8 a) the changes with temperature are more severe in the glaze ice range.

3.2 Turbulence, Noise, and Filtering

The results in Fig. 8 show the effect of ice on aircraft parameters as a function of atmospheric temperature and time for a given icing condition. However, these results do not include the effect of atmospheric turbulence and sensor noise that would be expected in an actual flight. Figures 9 and 10 add these effects to the clean and iced results for the Twin Otter.

The Dryden turbulence model from the FDC 1.3 code was used to model the atmospheric turbulence that might occur in an icing cloud. The turbulence was chosen such that aircraft z-accelerations of 0.13 g RMS with maximum variations up to +/- 0.5 g were encountered over the 5 minute flight. The noise was modeled assuming a band-limited white gaussian distribution with the amplitude set based upon the sensor uncertainties given by Ratvasky and Ranaudo.[12] The actual amplitudes for each variable were twice those given by Ratvasky and Ranaudo.[12]

In Fig. 9 a rectilinear, steady, level flight is considered with no icing. Three cases are shown: turbulence and sensor noise included, sensor noise and no turbulence, and no turbulence and no noise. The effect of sensor noise on angle of attack is small compared with the turbulence, which is a vertical gust, providing the majority of the deviation from the undisturbed signal. However, for the velocity most of the signal fluctuation comes from the sensor noise as the turbulence has only a small effect on the primarily axial velocity.

Figure 10 shows the clean and iced results turbulence and sensor noise and with filtering. The iced results vary from an η of 0 to 0.10 from 0 to 300 seconds. While the turbulence and noise cases in Fig. 11 were intended to simulate the raw sensor output that would be produced in an icing flight, it is expected that the sensor data would then be filtered to reduce the sensor noise and turbulence effects. The filtered data would then be used by the smart icing system's Ice Management System to analyze and characterize the effect of ice on the aircraft.

The filters used in Fig. 10 are low-pass Butterworth filters. The filter used for the velocity data is a 2nd order filter with a cut-off frequency of 0.17 Hz. The angle of attack data is filtered using a 5th order filter with a cut-off frequency of 0.1 Hz, while the elevator data uses a 3rd order filter with 0.13 Hz cut-off frequency.

The filters used assume the data is spaced at equal time intervals; however, the FDC code is set to generate data at non-uniform time steps to ensure accuracy. Better filtering can be expected in real time data, which will typically be sampled at regular time intervals, for which the standard filters are configured. The use of other filters dealing with white noise, such as Kalman filters, will also be explored in future studies. During actual flight, the data will have to be windowed, and this will cause a slight lag in the data output.

Considering the results in Fig. 10 the sensor noise and turbulence adds a significant uncertainty to the measurements. However, the filters chosen remove almost all of the high-frequency content. The icing effects are more easily assessed once the data are filtered. The filters shown here perform well, but even better filtering should be possible in the future.

3.3 Steady State Characterization

For the ice affects characterization function of the smart icing system, it is envisioned that both dynamic system identification and quasi-steady-state characterization will be used. During quasi-steady flight conditions the control inputs and disturbances are insufficient to excite the aircraft dynamics such that system identification techniques can not estimate the effect of ice on the stability and control derivatives in a robust manner. In these situations, a quasi-steady-state analysis is carried out to determine the onset of icing on an aircraft, in real-time, during flight.

An outline of the approach envisioned in the steady-state characterization is as follows:

1. Acquire flight data, using onboard sensors
2. Process aircraft data to obtain non-dimensional parameters in iced and equivalent clean conditions
3. Compare iced and clean values to determine "useful flight parameters" such as ΔV, $\Delta\alpha$, $\Delta\delta_E$, ΔC_D, and ΔC_h.
4. Set threshold values or use neural networks to determine onset of icing.
5. Analyze the Δ's and other sensor information to determine the type and location of ice accretion and the potential safety hazards

As an example of using thresholds to sense the presence of ice accretion consider the changes in V, α, δ_e predicted in Fig. 8. Table 2 shows the time in seconds, for the 5 atmospheric temperatures simulated, until the change exceeds a certain threshold value. The thresholds chosen are arbitrary, but not unrealistic values. In each case the time to sense the α and δ_e changes is similar with the velocity change exceeding the threshold in about one half the time. For example at T = 20°F, a 1 ft/s change in velocity is seen in 25.2 seconds. If a higher threshold of 2 ft/s is assumed it takes 36.6 seconds to exceed this value for this particular icing encounter. The times in Table 2 give a first estimate on the times that may be required to sense and begin to characterize icing effects from steady-state parameters.

3.4 Other Icing Encounters

In Fig. 11 the degradation due to icing in a level standard rate turn is compared to that in steady, level rectilinear flight. Here the standard rate turn is intended to represent part of a holding pattern, but it could also be representative of maneuvering during climb out or landing approach. The turn case will be referred to as a hold in this paper. In both cases, the flight is level and at constant power. For the hold the turn rate is 3 deg. per second. Here the velocity has been matched at 230 ft/s and the altitude is 6560 ft. All of the other parameters for the Twin Otter are the same as before including η varying from 0 to 0.10 from 0 to 300 seconds. Figure 11 shows the predicted velocity, angle of attack, elevator deflection, aileron deflection and rudder deflection required during the icing encounter in cruise or hold condition. In each of these cases, the effect of the ice on the flight parameters during the hold is more severe. This is due to the increased lift required in the hold and as a result larger power, angle of attack, and elevator deflection. For example consider the angle of attack. At time t = 0 the angle of attack is about 1.2° for rectilinear flight and about 1.5° in the turn. However, with ice the rectilinear case increases to 2.4° in 300 seconds while the turn case increases to 3.2°. Therefore, the increase in angle of attack for the hold case is 1.7° while only 1.2° for the rectilinear flight case. So the hold case increases the change in the flight

variables and as a result the sensitivity of the aircraft to icing effects. This could potentially improve the systems ability to sense icing when the aircraft is maneuvering.

It is desirable to be able to detect which parts of the aircraft have the most severe icing effects. For example due to the known safety hazard with tail ice, it would be desirable to be able to distinguish the case with horizontal tail ice from the ice over the entire aircraft.

Figure 12 shows the angle of attack, thrust required, and the elevator deflection when selected parts of the aircraft are iced. The derivatives used to represent the wing-ice, tail-ice and all aircraft ice are listed in Table 1. In each case the aircraft is at a constant velocity of 230 ft/s and a constant altitude of 6560 ft which are maintained by the autopilot. Again, the icing cloud simulated is such that after 300 seconds, the ice accretion is represented by $\eta = 0.10$.

In Fig. 12 the changes in α and δ_e are much smaller than in the previous simulations. Previously the power was held constant and as the drag increased due to the ice accretion, the aircraft slowed down. To maintain level flight the aircraft had to increase α to increase the lift coefficient and then add more elevator to trim. Therefore, in the constant power case much of the α and δ_e change was directly due to the large drag increase. Here the velocity is held constant by the autopilot by increasing the aircraft thrust as the ice accretes. This maintains the same aircraft lift coefficient throughout the 5 minute encounter. Thus the changes in α and δ_e are much smaller and reflect primarily the changes in lift curve slope and elevator power due to the ice. Consider the constant velocity case of Fig. 12 a) where the α increases about 0.067° over the 300 second encounter. By contrast the same case at constant power from Fig. 11 shows a change in α of 1.2°.

The small changes seen in α and δ_e in the constant velocity case for the representative icing encounter simulated here indicates that it will be difficult to distinguish tail from wing icing in this case. Bragg et al.[3] discussed in an earlier paper the possibility of using a hinge-moment-based aerodynamic sensor to sense ice accretion effects on control surfaces. Further work on this concept has been presented by Bragg and Gurbacki[25] and the concept looks very promising. Such an aerodynamic sensor may be needed to distinguish wing from tail icing as well as provide information on control effectiveness. This concept will be explored in future research.

4.0 SUMMARY AND CONCLUSIONS

A method to study the effect of ice accretion on the flight dynamics of an aircraft has been developed. The method is used to evaluate a method for sensing ice accretion through the change in steady-state aircraft parameters. Conclusions from this study include:

1. The use of η_{ice} to provide a simple model to extrapolate limited iced aircraft flight data appears to work well.
2. The effect of ice on V, α, and δ_e for the constant power case are significant and at values that can potentially be used to distinguish and characterize the accretion. Much of the effect here is governed by the drag rise due to ice.
3. Atmospheric turbulence and sensor noise provide scatter in the sensor data that can be successfully filtered.
4. Flight maneuvers, such as a holding turn, increase the effects of ice and improve the potential for sensing.
5. Using steady-state data to distinguish tail from wing ice will be difficult in the constant velocity case where α and δ_e changes are small. Aerodynamic performance monitors, such as the proposed hinge-moment sensor, may be useful here.

5.0 ACKNOWLEDGEMENTS

This work was supported in part by NASA Glenn grant NAG 3-21235. The authors would like to thank Mr. Tom Bond, Mr. Tom Ratvasky and Dr. Mark Potapczuk of NASA Glenn for their contributions. This work was also supported by a Critical Research Initiatives grant from the University of Illinois at Urbana-Champaign. Several members of the Smart Icing Systems research group at Illinois contributed to this research including, Prof. Tamer Basar, Mr. Jim Melody, Prof. Nadine Sarter, and many others. The authors would also like to thank Shuvranshu Pokhariyal for his assistance with the data filtering routines.

6.0 RERENCES

[1] Bragg, M.B., "Aircraft Aerodynamic Effects Due To Large-Droplet Ice Accretions," AIAA Paper No. 96-0932, Reno, NV, Jan. 1996.

[2] Bradley, J., Anderson, A., and Sivier, K., "The Impact of Smart Icing Systems on Commuter Aircraft," AIAA Paper No. 2000-0362, Reno, NV, Jan. 10-14, 2000.

[3] Bragg, M.B., Perkins, W.R., Sarter N.B., Basar, T., Voulgaris, P.G., Gurbacki, H.M., Melody, J.W. and McCray, S.A., "An Interdisciplinary Approach to

Inflight Aircraft Icing Safety," AIAA Paper No. 98-0095, Reno, NV, January 12-15, 1998.

[4] E. Schuchard, E., Melody, J., Perkins, W., Basar, T., and Voulgaris, P., "Detection & Classification of Aircraft Icing Using Neural Networks," AIAAPaper No. 2000-0361, Renŏ, NV, Jan. 10-14, 2000.

[5] Preston, G.M. and Blackman, C.C., "Effects of Ice Formation on Airplane Perfromance in Level Cruising Flight," NACA TN 1598, May 1948.

[6] Leckman, P.R., "Qualification of a Light Aircraft for Flight in Icing Conditions," SAE paper No. 710394, 1971.

[7] Ashenden, R. and Marwitz, J., "Turboprop Aircraft Performance Response to Various Environmental Conditions," AIAA Paper No. 97-0305, Reno, NV, Jan. 1997.

[8] Ranaudo, R.J., Mikkelsen, K.L., McKnight, R.C., and Perkins, P.J., "Performance Degradation of a Typical Twin Engine Commuter Type Aircraft in Measured Natural Icing Conditions," NASA TM83564 and AIAA 84-0179, Jan. 1984.

[9] Mikkelson, K.L., McKnight, R.C., and Ranaudo, R.J., "Icing Flight Research: Aerodynamic Effects of Ice and Ice Shape Documentation With Stereo Photography," NASA TM 86906 and AIAA 85-0468, Jan. 1985.

[10] R.J. Ranuado, et.al., The Measurement of Aircraft Performance and Stability and control After Flight Through Natural Icing Conditions," AIAA 86-9758, 1986.

[11] Ranaudo, R.J., Batterson, J.G., Reehorst, A.L., Bond, T.H. and O'Mara, T.M., "Determination of Longitudinal Aerodynaimc Derivatives Using Flight Data From an Icing Research Aircraft," NASA TM 101427 and AIAA 89-0754, Jan. 1989.

[12] Ratvasky T.P. and Ranaudo, R.J., "Icing Effects on Aircraft Stability and Control Determined from Flight Data," NASA TM 105977 and AIAA 93-0398, Jan. 1993.

[13] Bragg, M.B., "Aerodynamics of Supercooled-Large-Droplet Ice Accretion and the Effect on Aircraft Control," *Proceedings of the FAA International Conference on Aircraft Inflight Icing*, Volume II, DOT/FAA/AR-96/81,II, August 1996, pp. 387-399.

[14] Trunov, O.K. and Ingelman-Sundberg, M., "On the Problem of Horizontal Tail Stall Due to Ice," Report JR-3, The Swedish Sovjet Working Group on Scientific-Technical Cooperation in the Field of Flight Safety, 1985.

[15] Ratvasky, T.P., Van Zante, J.F., and Riley, J.T., "NASA/FAA Tailplane Icing Program Overview," AIAA Paper No. 99-0370, Reno, NV, Jan. 11-14, 1999.

[16] Karlsen, L.K. and Solberg, A., "Digital Simulation of Aircraft Longitudinal Motions With Tailplane Icing," KTH Aero Report 55, TRITA-FPT-043, ISSN 0280-1078, Dept. of Aeronautics, The Royal Institute of Technology, Stockholm, Sweden, Dec. 1983.

[17] Hiltner, D.W., "A Nonlinear Aircraft Simulation of Ice Contaminated Tailplane Stall," Ph.D. dissertation, The Ohio State University, 1998.

[18] Miller, R and Ribbens, W., "The Effects of Icing on the Longitudinal Dynamics of an Icing Research Aircraft," AIAA Paper No. 99-0636, Reno, NV, January 11-14, 1999.

[19] Miller, R. and Ribbens, W., "Detection of the Loss of Elevator Effectiveness Due to Aircraft Icing," AIAA Paper No. 99-0637, Reno, NV, January 11-14, 1999.

[20] Cook, D., "Relationships of Ice Shapes and Drag to Icing Condition Dimensionless Parameters," AIAA Paper No. 2000-0486, Reno, NV, Jan. 10-14, 2000.

[21] Olsen, W. Shaw, R., and Newton, J., "Ice Shapes and Resulting Drag Increase for a NACA 0012 Airfoil," NASA TM 83556, 1984.

[22] Bowden, D.T., "Effect of Pneumatic De-Icers and Ice Formations on Aerodynamic Character of an Airfoil," NACA Technical Note 3564, February, 1956.

[23] Hoak, D.E., et al, USAF Stabiltiy and Control Datcom, Flight Control Divsion, Air Force Flight Dynamics Laboratory, WPAFB, Ohio, 45433-0000, 1978, revised.

[24] Rauw, Marc, "FDC 1.3 – A SIMULINK Toolbox for Flight Dynamics and Control Analysis," 1998.

[25] Bragg, M.B. and Gurbacki, H., "Sensing Aircraft Icing Effects by Flap Hinge Moment Measurement," Paper No. Paper No. 99-3149, Proceeding of the 17th AIAA Applied Aerodynamics Meeting, Norfolk, June 28 – July 1, 1999, pp. 368-378.

Table 1: Non-dimensional Derivatives for Twin Otter in Clean and Iced ($\eta = 0.20$) Configurations.

	C_{Z0}	$C_{Z\alpha}$	C_{Zq}	$C_{Z\delta e}$	C_{X0}	K	C_{m0}	$C_{m\alpha}$	C_{mq}	$C_{m\delta e}$
clean	-0.380	-5.660	-19.970	-0.608	-0.041	0.052	0.008	-1.310	-34.200	-1.740
wing_ice	-0.380	-5.342	-19.700	-0.594	-0.050	0.053	0.008	-1.285	-33.000	-1.709
tail_ice	-0.380	-5.520	-19.700	-0.565	-0.046	0.053	0.008	-1.263	-33.000	-1.593
all iced	-0.380	-5.094	-19.700	-0.550	-0.062	0.057	0.008	-1.180	-33.000	-1.566

	$C_{Y\beta}$	C_{Yp}	C_{Yr}	$C_{Y\delta r}$	$C_{l\beta}$	C_{lp}	C_{lr}	$C_{l\delta a}$	$C_{l\delta r}$	$C_{n\beta}$	C_{np}	C_{nr}	$C_{n\delta r}$	$C_{n\delta a}$
clean	-0.6	-0.2	0.4	0.15	-0.08	-0.5	0.06	-0.15	0.015	0.1	-0.06	-0.18	-0.12	-0.001
all iced	-0.48	-0.2	0.4	0.138	-0.072	-0.45	0.06	-0.135	0.0138	0.08	-0.06	-0.169	-0.11	-0.001

Table 2. Time in seconds to exceed the threshold values from the icing simulations in Fig. 9.

	$\Delta\alpha$ (deg)		
Static T (°F)	0.1	0.2	0.5
0	97.581	146.583	265.650
10	58.027	84.084	140.613
20	46.429	66.924	109.332
25	53.559	77.481	128.238
29	175.949	283.117	---

	$\Delta\delta_e$ (deg)		
Static T (°F)	0.1	0.2	0.5
0	115.155	175.593	---
10	67.617	98.406	166.716
20	54.021	77.880	128.187
25	62.360	90.376	151.404
29	213.355	---	---

	ΔV (ft/s)		
Static T (°F)	1.0	2.0	5.0
0	52.140	75.966	129.120
10	31.449	45.729	75.273
20	25.179	36.617	60.159
25	29.030	42.207	69.426
29	88.091	132.253	243.507

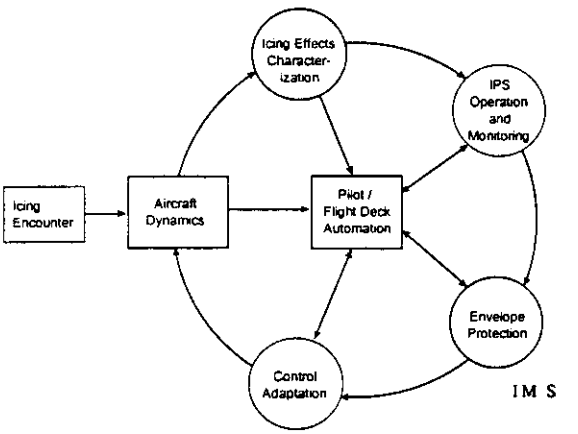

Fig. 1. Functional diagram of the smart icing system's ice management system.

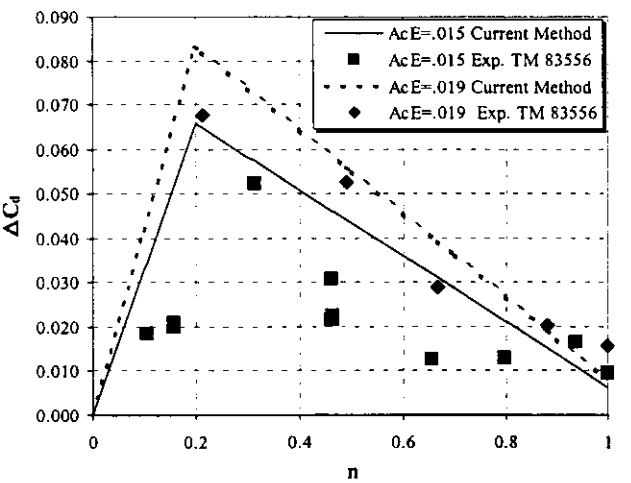

Fig. 2 Experimental and calculated values of the change in airfoil drag coefficient due to ice accretion with freezing fraction, *n*.

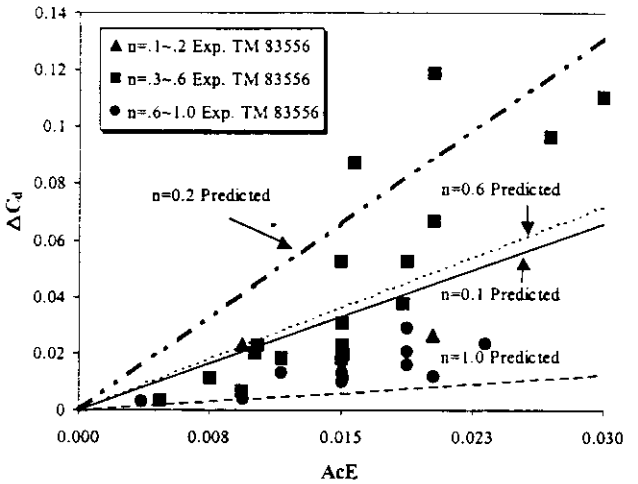

Fig.3 Experimental and calculated values of the change in airfoil drag coefficient due to ice accretion with A_cE.

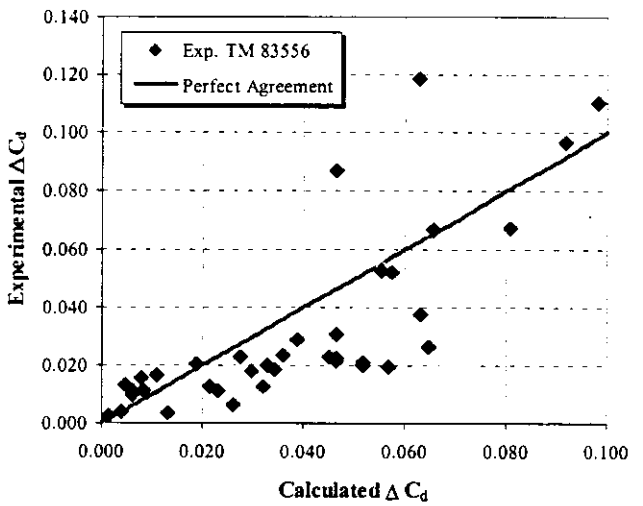

Fig. 4 Comparison of experimental and calculated airfoil ΔC_d values.

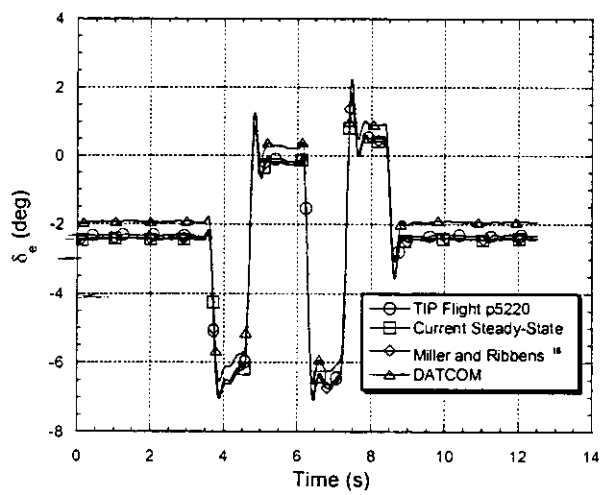

Fig. 5 Elevator doublet input to Flight Dynamics Code.

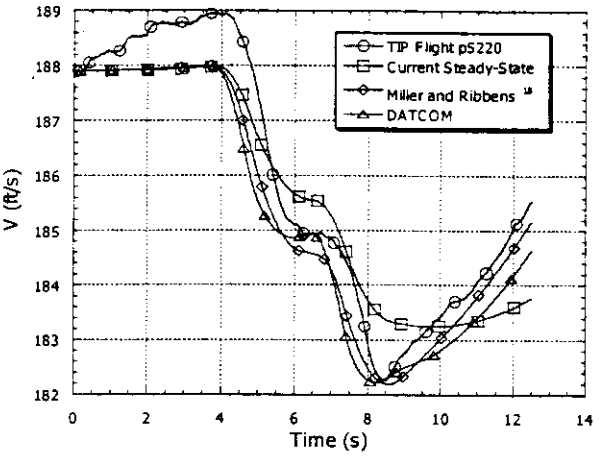

a) Velocity vs time

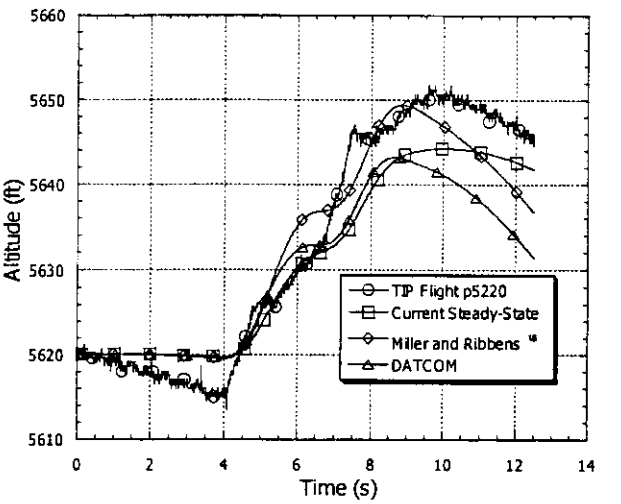

b) Altitude vs time

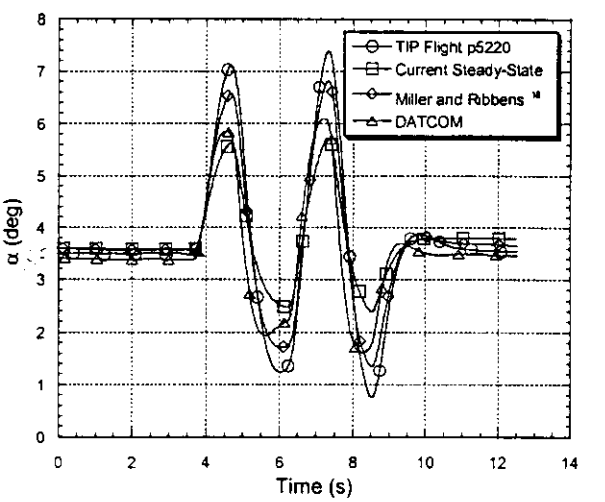

c) α vs time

Fig. 6. Calculated response of the Twin Otter to elevator double compared to experiment.

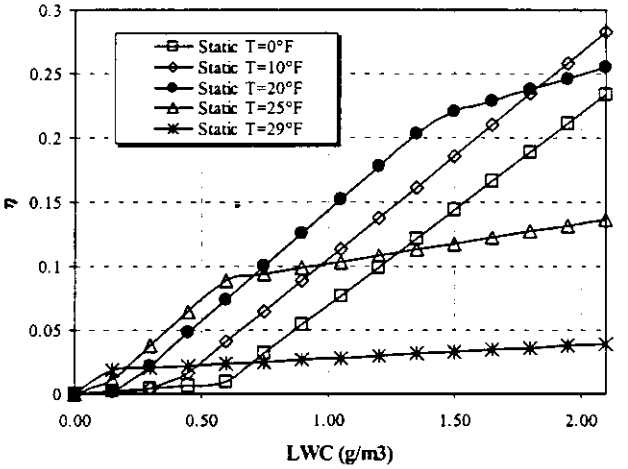

a) Effect of LWC on η

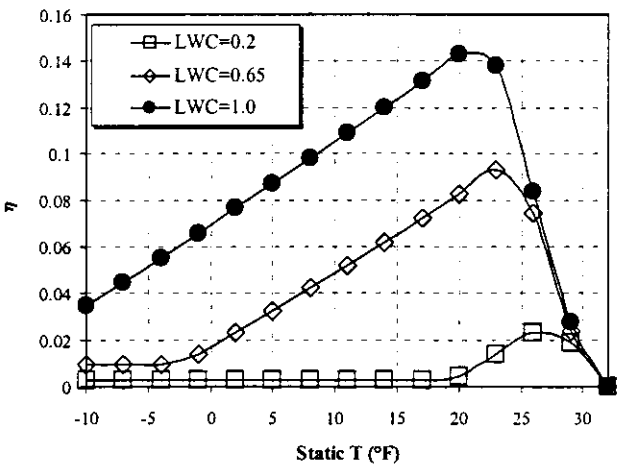

b) Effect of static temperature on η

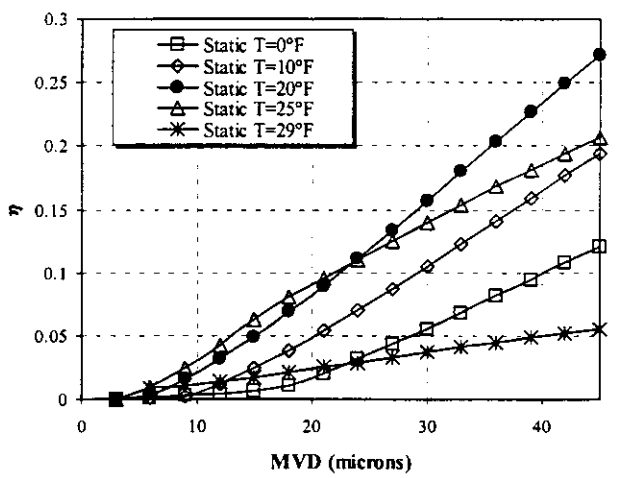

c) Effect of MVD on η

Fig. 7. Effect of cloud properties on the aircraft icing parameter η.

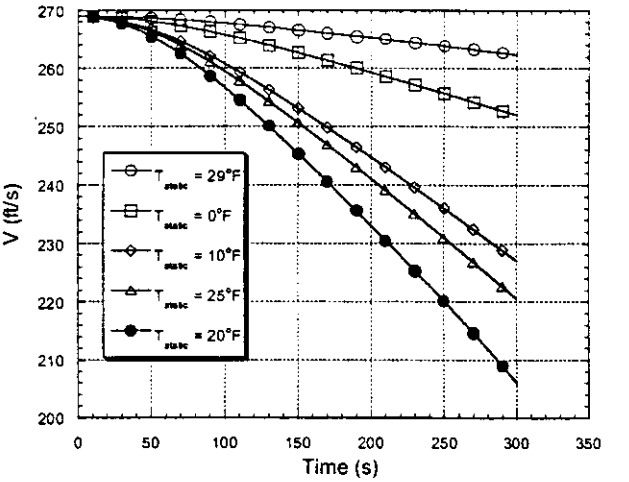

a) Velocity vs time

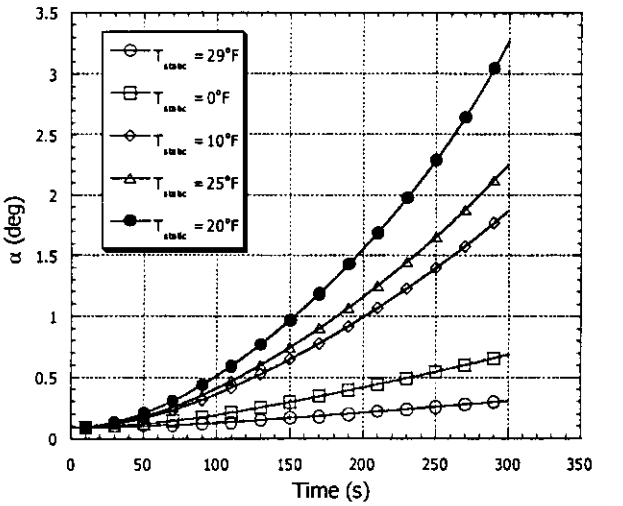

b) α vs time

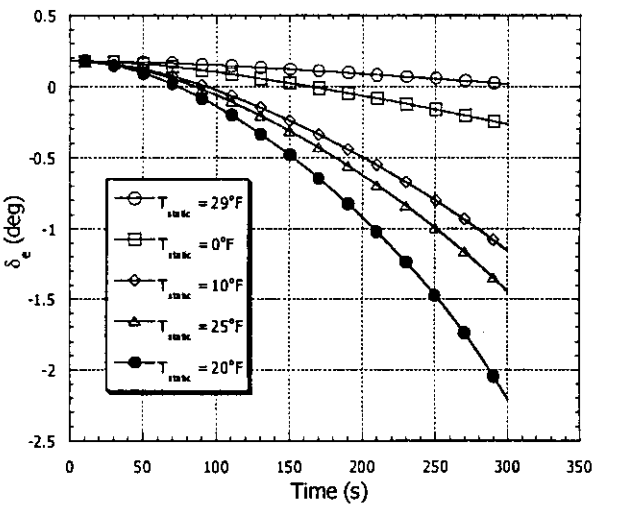

c) δ_e vs time

Fig. 8 Effect of temperature on cruise performance at constant power.

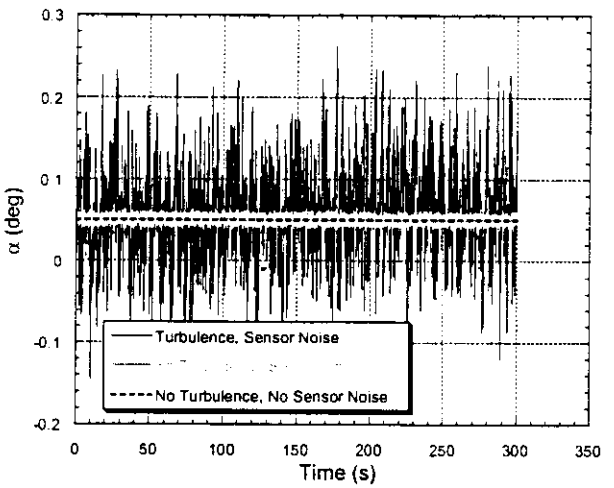

a) α vs time

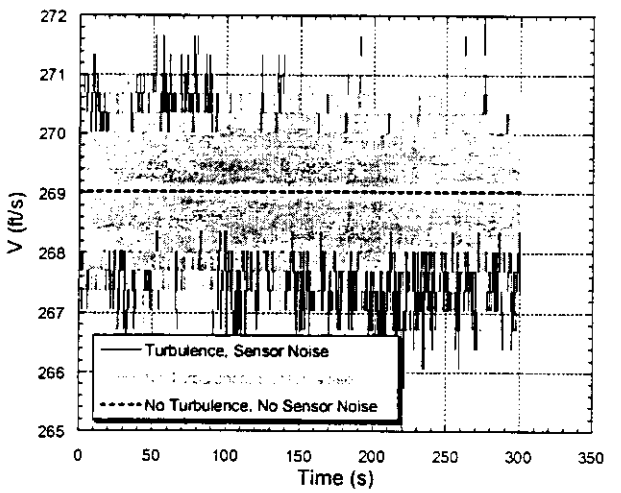

b) velocity vs time

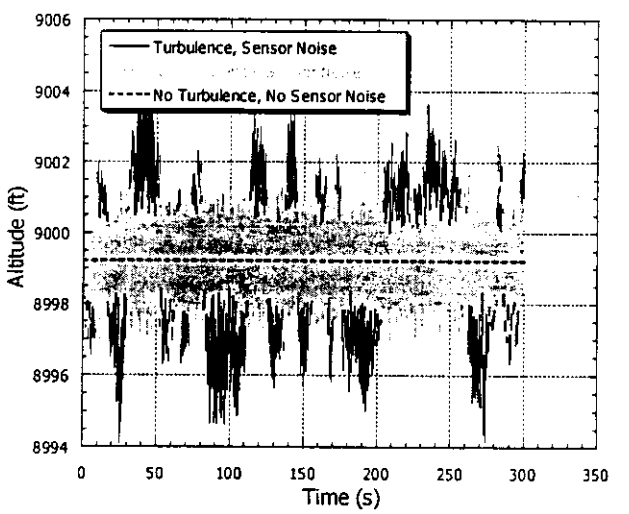

c) altitude vs time

Fig. 9. Effect of turbulence and noise on clean aircraft cruise parameters.

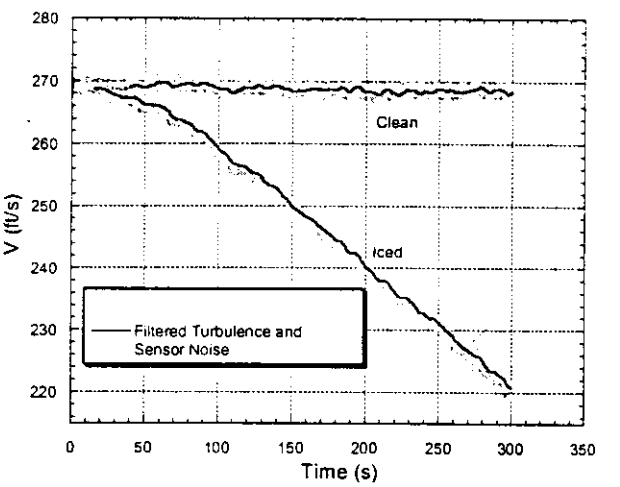

a) Velocity vs time

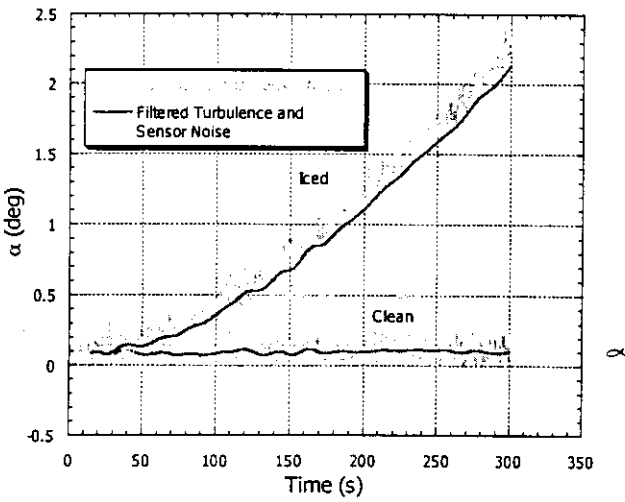

b) α vs time

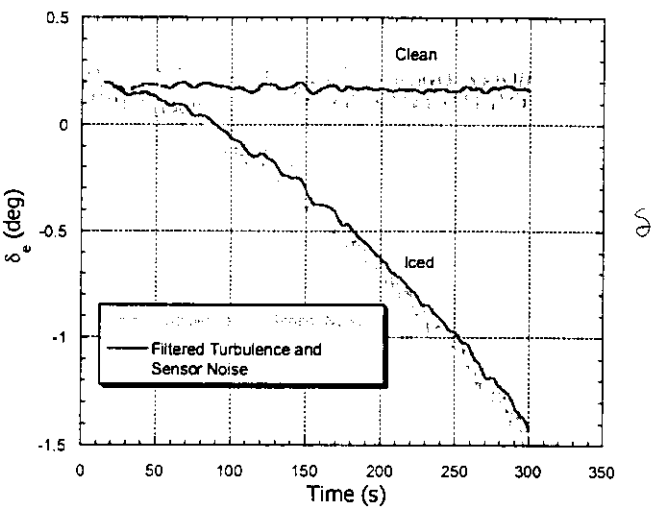

c) δ_e vs time

Fig. 10. Clean and iced (η = 0. to 0.10) performance at constant power with and with out filtering.

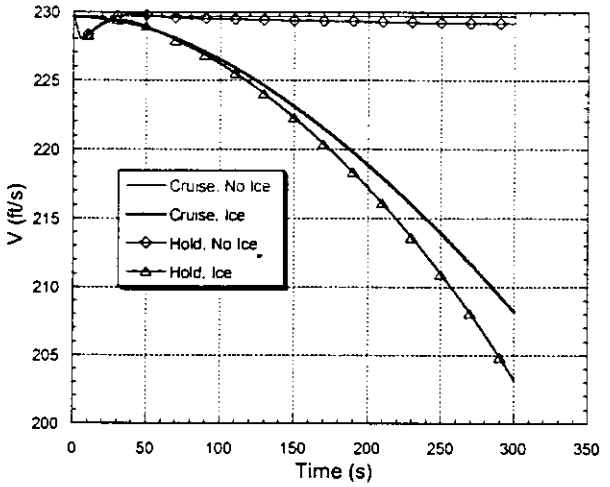

a) Velocity vs time

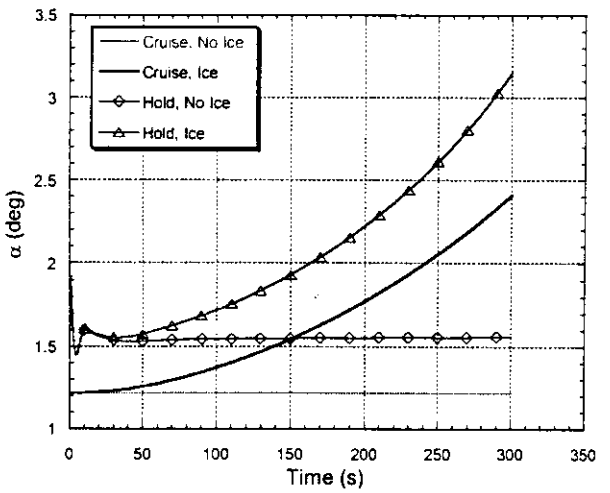

b) α vs time

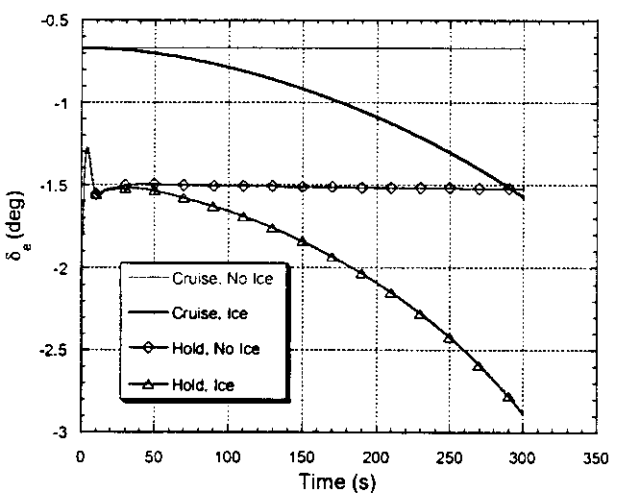

c) δ_e vs time

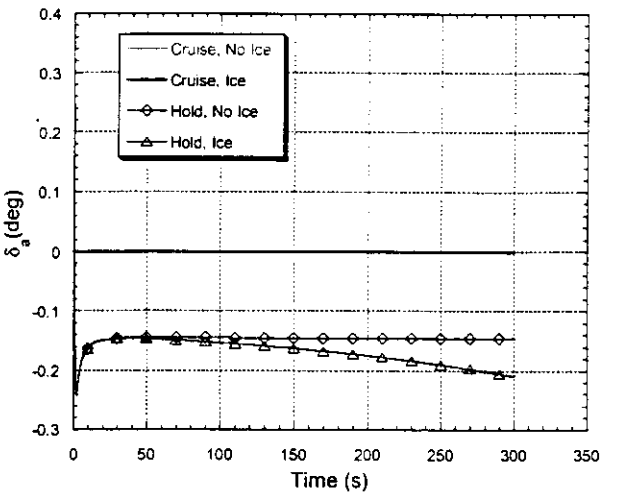

d) Aileron deflection,δ_a vs time

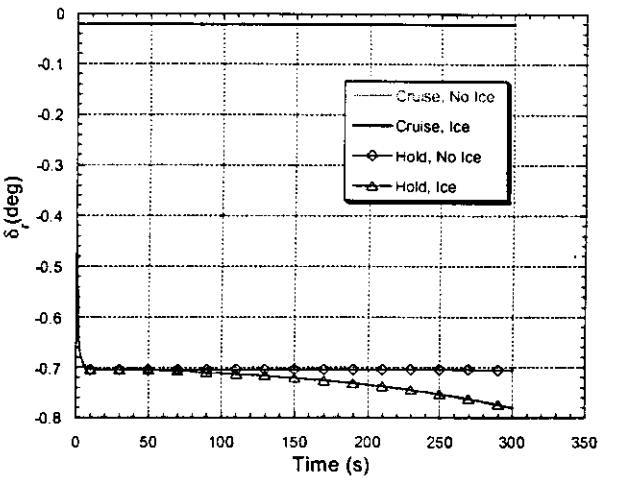

e) Rudder deflection,δ_r vs time

Fig. 11 Aircraft performance clean and iced (η = 0. to 0.10) in a holding turn and cruise at constant power. V = 230 ft/s and h = 6560 ft.

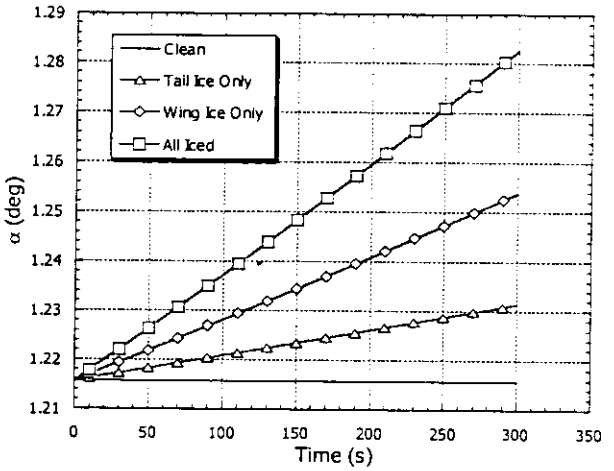

a) α vs time

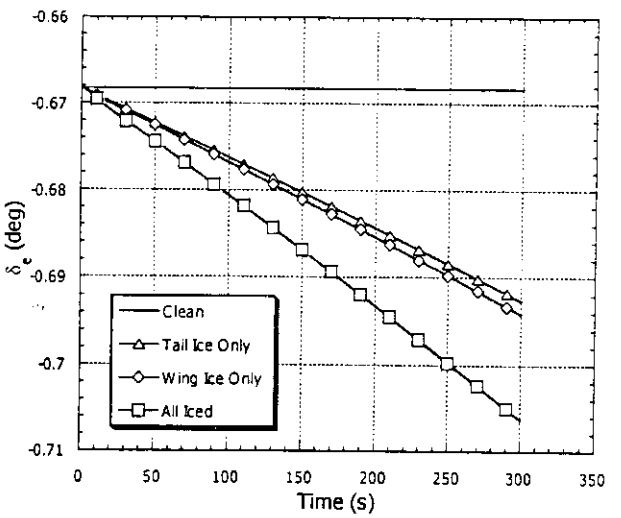

b) δ_e vs time

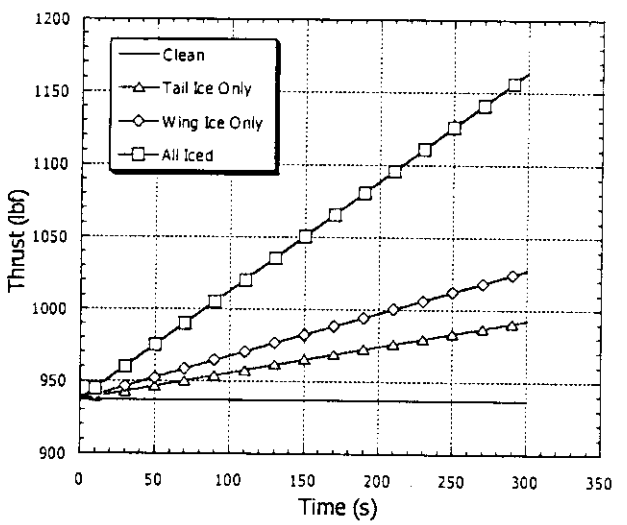

c) Thrust vs time

Fig. 12 Effect of ice (η = 0. to 0.10) on wing, tail, all iced in cruise at constant velocity. V = 230 ft/s and h = 6560 ft.